analytical chemistry

Article

Nanoparticle Enhanced Laser Induced Breakdown Spectroscopy for microdrop analysis at sub-ppm level.

Alessandro De Giacomo, Can Koral, Gabriele Valenza, Rosalba Gaudiuso, and Marcella Dell'Aglio

Anal. Chem., **Just Accepted Manuscript** • DOI: 10.1021/acs.analchem.6b00324 • Publication Date (Web): 23 Apr 2016

Analytical Chemistry is published by the American Chemical Society. 1155 Sixteenth Street N.W., Washington, DC 20036

Nanoparticle Enhanced Laser Induced Breakdown Spectroscopy for microdrop analysis at sub-ppm level.

Alessandro De Giacomo* [1,2], Can Koral[1], Gabriele Valenza[1,2] Rosalba Gaudiuso[1,2], Marcella Dell'Aglio[2].

1. University of Bari, Department of Chemistry, Via Orabona 4, 70126 Bari-Italy

2. CNR-NANOTEC, Via Amendola 122/D, 70126 Bari-Italy

Abstract

In this paper, Nanoparticle Enhanced Laser Induced Breakdown Spectroscopy (NELIBS) was applied to the elemental chemical analysis of micro-drops of solutions with analyte concentration at sub-ppm level. The effect on laser ablation of the strong local enhancement of the electromagnetic field allows enhancing the optical emission signal up to more than one order of magnitude, enabling LIBS to quantify ppb concentration and notably decreasing the Limit Of Detection (LOD) of the technique. At optimized conditions it was demonstrated that NELIBS can reach an absolute LOD of few pg for Pb and 0.2 pg for Ag. The effect of field enhancement in NELIBS was tested on biological solutions such as protein solutions and human serum, in order to improve the sensitivity of LIBS with samples where the formation and excitation of the plasma are not as efficient as with metals. Even in these difficult cases, a significant improvement with respect to conventional LIBS was observed.

Key words: Laser Induced Breakdown Spectroscopy (LIBS), Nanoparticle Enhanced Laser Induced Breakdown Spectroscopy (NELIBS), microdroplet, ppb level.

1. Introduction

Laser Induced Breakdown Spectroscopy (LIBS) is an analytical technique for elemental chemical analysis based on the optical emission signal of the plasma produced by laser-sample interaction [1,2]. Its main peculiarities are: easy set-up, multielemental analysis (including light elements), fast response and no or minimum sample treatment. In the last decades, thanks to these advantages, the use of LIBS has been growing in research and industrial laboratories for a wide range of applications, which include cultural heritage, geology, quality control of industrial products, biology etc [2]. The growing interest on this technique is pushing researchers to develop different methods for decreasing the Limit Of Detection (LOD) and improving the reproducibility [3].

Two approaches are possible to pursue the analysis of liquid solutions by LIBS: the first is directly performing LIBS of the solution itself [4], the second one is to transfer to or convert the liquid into a solid phase [3,5,6]. LIBS on the liquid surface provides poor reproducibility because of splashing and generation of surface waves during laser ablation, thus Double Pulse LIBS (DP-LIBS) in bulk solution is usually preferred. On the other hand, DP-LIBS also has some drawbacks, i.e., a comparatively high LOD (few ppm) and the need for large volumes of solution [4]. For these reasons, LIBS analysis of solutions in laboratory is generally carried out by drying drops of solution on a solid substrate [7,8]. With this approach it is possible to reach LOD in the range of several hundreds of ppb, depending on the volume of the droplet and number of signal accumulation. In this paper we propose a new method based on the use noble metal Nanoparticles (NPs) for enhancing the LIBS signal using a single laser shot. The use of nanostructures as ‘spectroscopic enhancers’ is receiving a growing interest for several applications in spectroscopy, microscopy and sensing [9-11] and we have recently demonstrated, for the first time, its application also for LIBS analysis of metallic samples, providing an impressive signal enhancement up to two orders of magnitude [12]. In the latter technique, the effect of the coupling between the electromagnetic field of the laser and the one induced on the surface plasmons of the NPs [13-15] causes the emission signal to dramatically increase, with a LOD decrease of up to two orders of magnitude with respect to LIBS. The main advantage of this technique, that we named Nanoparticle-Enhanced LIBS (NELIBS), is that the sample preparation in principle is very straightforward as it only requires to deposit a certain amount of NPs on the sample surface. In the simplest case this can be done just by drying a droplet of a colloidal solution of Au- or Ag-NPs on the sample to be analyzed [12]. On the other hand, the aim of this paper is to analyze liquid solutions by transporting in a stable plasma phase less than 1 ng of analyte, deposited on a solid substrate by drying 1 μl of solution. This means that the field enhancement phenomenon should not involve the substrate where NPs have been deposited, in order to avoid that a portion of the laser energy is spent for vaporizing the substrate, and that the atomized substrate further dilutes the sample in the plasma phase. For this reason NPs have to be deposited on an insulating substrate, so that they act like a support for the analytes contained in the microdrop of sample solution. When the coupling between the laser electromagnetic field and the one induced on the surface plasmons of the NPs takes place, both the deposited sample and the NPs themselves are completely vaporized. The result of the laser ablation is then the formation of an intense plasma consisting of the sample elements, as well as of atoms and ions from the NPs. This approach makes it possible to detect and quantify sub-ppm level concentrations with a single laser shot and using a minimum volume of solution. This perspective appears extremely appealing for applications, such as forensic or medical ones, where fast response, small sample volume and low concentrations are major issues.

2. Experimental section.

The experimental set-up used in this work is a typical LIBS system: the laser induced plasma was produced with a Nd:YAG laser (Quantel Q-smart 850) at 1064 nm, 6 ns amplitude and energy up to 800 mJ, suitably focused on the sample with a biconvex lens of 100 mm focal length. The emission light was collected with a spectroscopic system consisting of a Czerny-Turner spectrograph (JY Triax 550) coupled with an ICCD (JY 3000) which was synchronized with the Pockels cell of the laser source with a pulse generator (Stanford DG 535). The plasma emission was steered and focused on the entrance slit of the spectrograph with a 45° mirror and a system of lenses, comprising three quartz lenses, in order to reduce the image size to 1/3. For plasma image acquisition, the plasma emission was directly focused on the ICCD coupled with a telephoto system. In all the spectroscopy experiments the detection times were: delay time from the laser pulse 800 ns and gate width 10 µs (virtually an integrated time LIBS measurement). In the case of imaging measurements, the delay was varied with a step of 500 ns and the gate width was 500 ns. For the LIBS experiment, 1 µl of sample solution was deposited on an inert substrate (glass, silicon or Teflon were used), while in the case of NELIBS, a bed of Au-NPs was deposited on the substrate before the sample solution, by drying 1 µl of a colloidal solution (the concentrations used were in the range 10^{-4}-10^{-1} mg/ml). As an example, Fig.1 shows the absorption spectrum and the SEM image of a glass substrate after the deposition of 1 µl of a 2 10^{-2} mg ml^{-1} of Au NP dispersion before the NELIBS measurement. It is clear that, although part of the NPs aggregate in small bidimensional clusters, the NP film still maintains a significant plasmonic activity. The latter information is extremely important in order to search for suitable conditions for an efficient local enhancement of the electromagnetic field. After the substrate preparation, a micro-drop of solution was deposited on the NP coating and dried by air flow. The diameter of the dried drop, both in the case of LIBS and NELIBS, was around 2 mm, thus, in order to irradiate and evaporate the entire sample, the focused laser spot was made equal to 2.5 mm. In these focusing conditions, in the case of the glass substrate without NPs, there is no laser-glass coupling and the beam passes without ablating the glass. When either the solution sample or the sample plus NPs are deposited on the glass surface, a plasma is induced, which mainly involves the deposited material. By optical microscopy it was possible to establish that no visible damage was induced on the glass, though in NELIBS spectra some emission lines coming from elements of the substrate were present, suggesting that although from the physical point of view the interaction of the laser with the substrate is negligible, when the plasma is produced, the most superficial layers of the substrate can be evaporated. This implies that special caution should be taken in the selection of the analyte emission lines, in order to avoid interferences from the glass substrate. Measurements were carried out in single shot mode, and to improve the reproducibility each measurement was repeated 8 times and then averaged. The peaks corresponding to the transitions of interests were fitted by Voigt curves, in order to determine the effective peak area, to subtract the background (due to the radiative recombination) and to deconvolute the peak from the adjacent ones (if any). The line intensity, determined as described, was then used as the analytical signal, without any normalization procedure. All the investigated emission lines were selected in order to avoid interferences with signals from impurities, and with relative intensity as high as possible. The used transitions are: Pb I at 405.78 nm, Ag I at 328.07 and 338.29 nm, and the Li I doublet at 670.78 – 670.79 nm.

Sample solutions with different concentrations were obtained by diluting standard solutions of $PbCl_2$, $Pb(NO_3)_2$ and $AgNO_3$. The $PbCl_2$ and $AgNO_3$ solutions were prepared by dissolving the necessary amount of salt in milli-Q water (resistivity: 18.2 MΩ cm at normal conditions), obtained with Milli-Q® Integral Water Purification System, while the $Pb(NO_3)_2$ was prepared by diluting a standard 1.00 g/L solution with milli-Q water. $PbCl_2$ (98%, CAS Number 7758-95-4) and $AgNO_3$ (ACS reagent >99 %, CAS Number 7761-88-8) salts, the $Pb(NO_3)_2$ solution (as lead for atomic spectroscopy standard concentrate 1.00 g, Pb 1.00 g/L, analytical standard, CAS Number 10099-74-8), and Human Serum (from human male AB plasma, USA origin, sterile-filtered, H4522-20ML) were purchased from Sigma Aldrich. The protein “Reaction Center” (RC) from the purple bacterium Rhodobacter sphaeroides was isolated and purified according to Gray et al. [16]. In all preparations, the ratio of the absorption at 280 and 800 nm was between 1.2 and 1.3. This isolation procedure provides RCs with a QB content of about 60%. RC was suspended in 10 mM Tris-HCl buffer at pH=8.00, Lauryl-Dimethyl-Amino-Oxide (LDAO) 0.025% (w/V), hereafter TL buffer. Ultrapure mQ water (Millipore) was used. After the functionality assay, the sample at Li concentration equal to 1.00 M, was dialyzed (3kDa cut-off dialysis membrane) against TL buffer for about 24 hours with two changes of buffer (in any case the volume ratio was 1:100). Au colloidal solutions of various sizes (0.06 mg/ml in aqueous buffer, NanoComposix, Inc.), as well as Au NPs of different size produced by laser ablation in liquid as described in [17] were used for preparing the sample.

3. Discussion.

3.1 Fundamental aspects

The most attractive feature of NELIBS is that, thanks to the coupling of the electromagnetic field of the laser with the one induced on the surface plasmons of the NPs, a strong local enhancement of the electromagnetic field is obtained [13-15]. This phenomenon is related to the fact that the laser pulse induces coherent oscillation of the conduction electrons in small metallic particles, which in turn amplifies the incident electromagnetic field increasing the latter in the vicinity of the particle surface [18]. The particular interest of the local electric field enhancement in laser-based analytical techniques is that the effective intensity of the incident electromagnetic radiation results remarkably increased. As shown in detail in ref. [19], in the case of LIBS, where the crucial process for the ablation and plasma induction is the production of seed electrons, the local enhancement of the electromagnetic field appears extremely useful because it allows extracting electrons from the sample by field electron emission, simultaneously in multiple ignition points. The main result is a more efficient ablation and plasma excitation, and, in turn, an increase of the emission signal.

Fig.2 shows the intensity enhancement (determined as the ratio between NELIBS and LIBS intensity of Pb I at 405.78 nm), as a function of the concentration of NPs deposited on a glass substrate (i.e. NP surface density) together with 1 μl drop of a 2.5 ppm $PbCl_2$ solution. In analogy with what has been observed in the case of NELIBS of metals, there is a critical surface density at which an evident rise of the enhancement occurs [19]. At NP surface density beyond this critical value, the sharp increase of the electromagnetic field and the small tunneling barrier allows producing several seed electrons, thanks to the multiple ignition mechanism described above. If the surface density of Au-NPs is too high, a decrease of Pb I intensity is observed. This can be explained by two phenomena, i.e.: the formation of large NP aggregates which causes the electromagnetic field enhancement to decrease, and the excess of NP-generated Au species going into the plasma phase and diluting the analyte, whose emission intensity consequently decreases.

In order to optimize the electromagnetic field enhancement due to the NPs deposited on the surface, it is necessary to deposit the critical number of NPs on the substrate surface, in order to produce a layer of NPs with an optimal average distance between them [20]. This means that depending on the NP size, a different surface density of NPs is required. Fig.3 shows the critical surface density as a function of NP size, determined as the minimum surface density necessary to observe a sharp jump in emission intensity with respect to conventional LIBS at the same experimental conditions. For surface density of about one order of magnitude beyond the critical surface density of NPs, the intensity enhancement holds values higher than one order of magnitude, similarly to what has been observed previously with NELIBS of metals [12, 19]. It is important to underline that in the case of NELIBS of micro-drops for the detection of trace elements, the local enhancement of the electromagnetic field is not the only advantage of this technique, and two further advantages arise. First of all, analytes from the solution can adsorb on the NP surface, as NPs can act as natural nucleation seeds and growth sites for salts during the drop evaporation. This allows an optimal distribution of the analytes themselves on the ablative NP coating, which in turn ensures that they are completely ablated with a single laser shot. Moreover, when dealing with micro-drops and sub-ppm concentrations, the mass of analyte left after drying the solution is very low. This implies that with conventional LIBS the plasma would result very weak because only few material particles (i.e. atoms, ions and electrons) would be able to participate in its formation. For example, for 1 µl of solution containing 1 ppb of analyte , the mass of sample transported in the plasma phase is 1 pg, if we consider the laser ablation complete. This means that the number of particles in the plasma phase is in the order of 10^9, while in typical LIBS experiments, with ablated mass in the order of hundreds of nanograms, the number of particles is in the order of 10^{14}. The amount of particles in the plasma is crucial for the stability of the latter, because it is correlated to the number of electrons available for the excitation of the species in the plasma phase. The number of electrons is indeed directly proportional to the population in the upper level involved in the optical transition [21]. In this scenario, noble metal NPs work like an ideal buffer material, because they are easy to vaporize by laser irradiation (lower breakdown threshold with respect to the bulk material), their spectral interference is controllable by choosing the type of NPs (Au, Ag, Pt etc.), and their concentration in the plasma can be adjusted by varying the concentration of NPs in the colloidal solution (within the constrains of reaching the critical surface density as described previously). In other words, NPs on one hand increase the ablation and excitation efficiency thanks to field enhancement, and on the other hand feed the plasma with atoms, ions and electrons generated by the ablation of NPs themselves. The result of these two phenomena is that a much more intense and stable plasma is induced than in conventional LIBS of a dried micro-drop.

The global effect of NELIBS with respect to LIBS on plasma emission and dimension during 1 µl of 1 ppm $PbCl_2$ solution is illustrated in Fig.4 where typical emission images of LIBS and NELIBS are reported. This image was obtained by focusing the plasma emission directly on the ICCD with a telephoto system, and allows visualizing the emission spatial distribution in a color scale map, where the abscissa is the distance from the target, while the ordinate represents the radial dimension of the plasma. In the bottom of the figure is reported, with the same abscissa, the integrated emission intensity to highlight the emission enhancement of NELIBS with respect to LIBS. This Figure shows clearly that the plasma, during NELIBS, is brighter and spatially much more extended, thus providing a considerable advantage in emission detection for analytical purposes. It is also notable that, as a consequence of the different dynamics of plasma expansion, the most intense region in LIBS and NELIBS have different spatial locations.

3.2. Results

As mentioned previously, the emission signal of analytes from micro-drops of solutions deposited on a solid substrate can be strongly enhanced by coating the substrate with NPs. Fig.5 a) and b) show the comparison of a frame of NELIBS and LIBS spectra of 1 µl of 500 ppb $PbCl_2$ and $Pb(NO_3)_2$ aqueous solutions. In Figs.4, it is evident that in the NELIBS experiment the intensity of the Pb I emission line, both in the case of $PbCl_2$ and of $Pb(NO_3)_2$, is enhanced and clearly quantifiable, while with conventional LIBS, though present, it appears at the noise level. A comparison of NELIBS and LIBS calibration curves in the ppm range is reported in Fig. 6 a) and b). The NELIBS experiment displays an increase of the slope between 14 and 25 times, which implies an excellent sensitivity improvement with respect to LIBS. From the calibration curve slopes and the background standard deviation multiplied times a factor 3, we estimated the Pb LOD for NELIBS and LIBS, which respectively resulted of 2 ppb and 50 ppb (the respective Limit Of Quantitation, LOQ, were 6 ppb and 150 ppb). As an example the calibration curve of Pb at ppb level are reported in Fig.7 for the $PbCl_2$ solutions. It is important to underline that a quantitative measurement of Pb at the ppb level, using the Pb I transition at 405.78 nm, is only possible with NELIBS, because the LOQ of LIBS is 150 ppb, thus no quantification is possible below this level. The demonstrated possibility of measuring the concentration of elements at the ppb level in just 1 µl of solution and by a single laser shot is extremely attractive, also considering that LOD can be further improved just by increasing the volume of the sample droplet.

In order to confirm the results obtained with Pb salt solutions, we studied a solution of $AgNO_3$ with the same procedure. 1 µl of Au-NP solution was deposited and dried on a substrate, prior to depositing 1 µl of analyte solution ($AgNO_3$ 100 ppb). Fig. 8 shows the comparison between a NELIBS and LIBS spectral frame around the Ag I peaks at 328.07 and 338.29 nm . It is evident that this concentration is below the LOD of LIBS while it is clearly measurable by NELIBS.

Fig.9 reports the NELIBS calibration curve of Ag in 1 µl of $AgNO_3$ solution and clearly shows that concentrations as low as few hundreds of ppt can be measured. Fig.9 shows a measurable quantity of 300 ppt (with an estimated LOD of 200 ppt), while in the case of LIBS the LOQ was around 200 ppb. As it is possible to observe in the inset of Fig. 9, the major concern in the case of spectroscopic detection at very low concentration, is that contaminants may be on the same concentration level as the analytes, thus they may interfere with the spectral detection and affect the analysis. Contaminants are mainly impurities contained in the analyte solution and even in the NP dispersions, when they are produced with chemical synthesis methods. For this reason, cleaner techniques for NP production, such as Pulsed Laser Ablation in pure liquids, are strongly suggested for detection at ppb and sub-ppb level [22].

The use of NPs for LIBS analysis is useful not only for decreasing the detection limit, but also because it can play an important role in cases of samples difficult to vaporize or containing atoms with high ionization energy [2,3]. For example, proteins contain saturated bonds, which make them not conductive, and elements with high ionization energy (carbon, nitrogen, hydrogen and oxygen), thus upon laser irradiation they produce very weak plasmas. In such cases, the support of NPs, deposited as previously discussed, allows increasing plasma duration and emission intensity. To prove this, we show in Fig. 10 the comparison between NELIBS and LIBS spectra of 1 µl of solution of the Reaction Center from the purple bacterium Rhodobacter Shaeraides. This large protein was treated with alkali metal salts and after extensive dialysis, the native functionality was restored and all the cations removed, except Li. LIBS and NELIBS were used for detecting the residual Li content. When NPs were deposited, an emission enhancement of more than one order of magnitude was observed for Li signals at 671 nm. Thus, a calibration curve could be drawn to quantify the Li content, which resulted equal to 260 ppb.

Finally, we report one last example based on the observations previously reported about the LOD decrease and the possibility of exploiting NELIBS to avoid the plasma quenching in biological solutions. Fig. 11 reports the emission signal of Pb I in NELIBS spectra of 1 µl of artificially Pb-contaminated human serum. In this experiment 1µl of $PbCl_2$ solution with different concentrations (1000, 100, 10 ppm) was mixed with 100 µl of pure human serum, in order to obtain three solutions with Pb concentration of, respectively, 7.4 ppm, 0.74 ppm and 74 ppb. We can see that in this case, again with 1µl of solution, LIBS does not allow a clear detection of lead for concentration lower than 5 ppm, while with NELIBS Pb appears detectable down to 74 ppb. Although physiologically relevant concentration of Pb in serum is below 50 ppb, NELIBS shows an evident improvement with respect to LIBS, where the LOD in 1 µl of serum is at ppm level. This clearly shows the potential of NELIBS even in real cases of study, and considering that, by increasing the amount of analyzed solution, a further decrease in the NELIBS LOD can be reasonably expected, this result can be considered as a first step towards a wide range of medical and forensic applications.

4. Conclusion.

In this paper the use of nanoparticles as LIBS enhancers, previously demonstrated for metals, was tested for the elemental analysis of micro-drops of 1µl volume of liquid solutions, in single shot mode. An evident enhancement of the analyte emission intensity was found when the micro-drop of solution was deposited on a substrate covered with Au-NPs. In agreement with our previous studies, the NELIBS enhancement with respect to conventional LIBS was ascribed to three phenomena: field enhancement due to the coupling of the electromagnetic field of the laser with the one induced on the NP surface plasmon (main effect); adsorption of analytes on the NP surface; increase of the number density of particles in the plasma phase as a consequence of the ablation of NPs. We tested NELIBS with aqueous solutions of Pb and Ag salts, and found absolute LOD of 2 and 0.2 pg, respectively. The effect of NPs was studied also in the case of proteins and human serum solutions, which were artificially contaminated by metal ions. NELIBS shows interesting advantages also in these cases, because the initial higher energy input due to the field enhancement allows a better excitation of the plasma with respect to LIBS also when the sample contains atoms with high ionization energy. Particularly promising is the possibility of metal detection in micro-drops of human serum because it opens the path to transfer NELIBS to real case applications, such as in medical and forensic science. Further investigation on sample preparation based on nanotechnological approaches can be expected to further improve the capabilities of NELIBS in terms of sensitivity and accuracy.

References:

[1] D.W. Hahn, N. Omenetto, Laser Induced Breakdown Spectroscopy (LIBS), Part II: Review of Instrumentation and Methodological Approaches to Material Analysis and Applications to Different Field, Applied Spectroscopy (2012) 66/4, 347-419.

[2] A.W. Miziolek, V. Palleschi, I. Schechter (Eds), “Laser Induced Breakdown Spectroscopy”, Cambridge University Press 2006.

[3] S.C. Jantzi , V. Motto-Ros, F. Trichard , Y. Markushin, N. Melikechi, A. De Giacomo, Sample treatment and preparation for laser-induced breakdown spectroscopy, Spectrochimica Acta Part B 115 (2016) 52–63.

[4] A. Matsumoto, A. Tamura, R. Koda, K. Fukami, Y. H. Ogata, N. Nishi, B. Thornton, T. Sakka, On-Site Quantitative Elemental Analysis of Metal Ions in Aqueous Solutions by Underwater Laser-Induced Breakdown Spectroscopy Combined with Electrodeposition under Controlled Potentia, Anal. Chem. 2015, 87, 1655−1661.

[5] F.F. Al-Adel, M.A. Dastageer, K. Gasmi, and M.A. Gondal, Optimization of a Laser Induced Breakdown Spectroscopy Method for the Analysis of Liquid Samples, J. Appl. Spectrosc., 80 (2013) 767-770.

[6] X. Wang, Y. Wei, Q. Lin, J. Zhang, and Y. Duan, Simple, Fast Matrix Conversion and Membrane Separation Method for Ultrasensitive Metal Detection in Aqueous Samples by Laser-Induced Breakdown Spectroscopy, Anal. Chem., 87 (2015) 5577-5583.

[7] E. M. Cahoon and J.R. Almirall, Quantitative Analysis of Liquids from Aerosols and Microdrops Using Laser Induced Breakdown Spectroscopy, Anal. Chem. 2012, 84, 2239−2244.

[8] M.A. Aguirre, E.J.Selva, M.Hidalgo, A. Canals, Dispersive liquid–liquid microextraction for metals enrichment: A useful strategy for improving sensitivity of laser-induced breakdown spectroscopy in liquid samples analysis, Talanta 131 (2015) 348–353.

[9] Nie, S.; Emory, S. R., Probing Single Molecules and Single Nanoparticles by Surface-Enhanced Raman Scattering. Science 1997, 275, (5303), 1102-1106.

[10]F.C. Adams, C.Barbante, Nanoscience, Nanotechnology and Spectrometry, Spectrochimica Acta Part B (2013) 86, 3-13.

[11] Kühn, S., Håkanson, U., Rogobete, L. & Sandoghdar, V. Enhancement of single-molecule fluorescence using a gold nanoparticle as an optical nanoantenna. Phys. Rev. Lett. 2006, 97: 017402.

[12] A. De Giacomo, R. Gaudiuso, C. Koral, M. Dell'Aglio, O. De Pascale, Nanoparticles Enhanced Laser Induced Breakdown Spectroscopy on metallic samples, Analytical Chemistry (2013) 85, 10180-10187.

[13] T. Turker, F. Robicheaux, Dichotomy between tunneling and multiphoton ionization in atomic photoionization: Keldysh parameter γ versus scaled frequency Ω, Physical Review A (2012) 86, 053407, 1-10

[14] F. Schertz, M. Schmelzeisen, M. Kreiter, H.J. Elmers, G. Schonhense, Field Emission Effect Generated by the Near Field of Strongly Coupled Plasmons, Physical review Letters (2012) 108, 237602, 1-5.

[15] S. M. Teichmann, P. Rácz, M. F. Ciappina, J. A. Pérez-Hernández, A. Thai, J. Fekete, A. Y. Elezzabi, L. Veisz, J. Biegert, P. Dombi, Strong-field plasmonic photoemission in the mid-IR at <1 GW/cm^2 intensity, Scientific Reports (2015) 5, 7584.

[16] K..A Gray, J. Wachtveil, J. Breton, D. Oesterhelt, Initial characterization of site-directed mutants of tyrosine M210 in the reaction centre of Rhodobacter sphaeroides, EMBO J. 1990, 9(7), 2061-2070

[17] M. Dell'Aglio, R. Gaudiuso, R. ElRashedy, O. De Pascale, G. Palazzo, A. De Giacomo, Collinear double pulse laser ablation in water for the production of silver nanoparticles, Phys.Chem. Chem. Phys., 2013, 15, 20868

[18] A. Grubisic,, E. Ringe, C. M. Cobley, Y. Xia, L. D. Marks, R. P. Van Duyne,D. J. Nesbitt, Plasmonic Near-Electric Field Enhancement Effects in Ultrafast Photoelectron Emission:

Correlated Spatial and Laser Polarization Microscopy Studies of Individual Ag Nanocubes, Nano Lett. 2012, 12 (9), 4823-4829

[19] A. De Giacomo, R. Gaudiuso, C. Koral, M. Dell'Aglio, O. De Pascale, Nanoparticle Enhanced Laser Induced Breakdown Spectroscopy: Effect of nanoparticles deposited on sample surface on laser ablation and plasma emission, Spectrochimica Acta Part B 98 (2014) 19–27.

[20] Mark K. Kinnan and George Chumanov, Plasmon Coupling in Two-Dimensional Arrays of Silver Nanoparticles: II. Effect of the Particle Size and Interparticle Distance, J. Phys. Chem. C, 2010, 114, 7496–7501.

[21] A. De Giacomo, M. Dell'Aglio, O. De Pascale, V. Palleschi, C. Parigger , A. Wood (2014). Plasma Processes and emission spectra in Laser Induced Plasmas: a point of view. Spectrochimica Acta Part B (2014) 180-188.

[22] S. Barcikowski, G Compagnini, Advanced nanoparticle generation and excitation by lasers in liquids, Phys. Chem. Chem. Phys., 2013, 15, 3022.

Figure Captions

FIG.1: Absorption spectrum and SEM image of a glass substrate after the deposition of 1μl of 2 10^{-2} mg ml^{-1} Au-NPs before the NELIBS measurement.

FIG.2: NELIBS spectral line enhancement of Pb I at 405.7 nm as a function of surface density of Au-NPs (diameter of 10 nm). The sample solution was 1 μl of 1 ppm $PbCl_2$, laser fluence 16.3 J cm^{-2}.

FIG.3: Critical surface density and corresponding number of NPs deposited on substrate surface as functions of NP diameter in NELIBS experiment.

FIG.4: Total emission images of LIBS and NELIBS plasma of 1 μl of 1 ppm $PbCl_2$ (delay time from the laser pulse: 1.3 μs, gate width: 500 ns, laser fluence: 16.3 J cm^{-2}). In the case of NELIBS, 1 μl of Au-NPs solution 0.04 mg ml^{-1} was used.

FIG.5: Comparison between the NELIBS and LIBS spectral line of Pb I (405.7 nm) for 1 μl of 500 ppb a) $PbCl_2$ and b) $Pb(NO_3)_2$ solutions. Experimental conditions: laser fluence 16.3 J cm^{-2}, 1 μl of 0.04 mg ml^{-1} Au-NPs.

FIG.6: Calibration curve of Pb in the range of 0.5 ppm to 8 ppm in the case of a) $PbCl_2$ and b) $Pb(NO_3)_2$. Experimental conditions: 1μl of sample solution, laser fluence 16.3 J cm^{-2}, 1 μl of Au-NPs 0.04 mg ml^{-1}.

FIG.7: Calibration curve of Pb in the range of 0 ppb to 250 ppb in the case of $PbCl_2$. Experimental conditions: 1μl of sample solution, laser fluence 16.3 J cm^{-2}, 1 μl of Au-NPs 0.04 mg ml^{-1}.

FIG.8: Comparison between the NELIBS and LIBS spectral line of Ag I (328.07 nm), for 1 μl of 100 ppb $AgNO_3$ solution. Experimental conditions: 1 μl of sample solution, laser fluence 12. J cm^{-2}, 1 μl of Au-NPs (diameter of 20 nm) 0.03 mg ml^{-1}.

Fig.9: Calibration curve of Ag in the concentration range between 0 and 6 ppb. In the inset the spectral line of Ag I at 328.07 nm at Ag concentrations of 11.7 ppb and 0.35 ppbare shown. Experimental conditions: 1 μl of $AgNO_3$ sample solution, laser fluence 12. J cm^{-2}, 1 μl of Au-NPs (diameter of 20 nm) 0.03 mg ml^{-1}.

FIG.10: Comparison between the NELIBS and LIBS signal of Li in 1 µl of solution of the protein Reaction Center (RC) from the purple bacterium Rhodobacter sphaeroides at concentration 10^{-5} M. Experimental conditions: laser fluence 20.4 J cm^{-2}, 1 µl of Au-NPs (diameter of 20 nm) 0.06 mg ml^{-1}.

FIG.11: NELIBS spectra of human serum artificially contaminated with $PbCl_2$ at different concentration: 74 ppb, 740 ppb and 7400 ppb. The detector gain is different for each measurement in order to maximize the emission signal. Experimental conditions: laser fluence 20.4 J cm^{-2}, 1 µl of Au-NPs (diameter of 20 nm) 0.08 mg ml^{-1}.

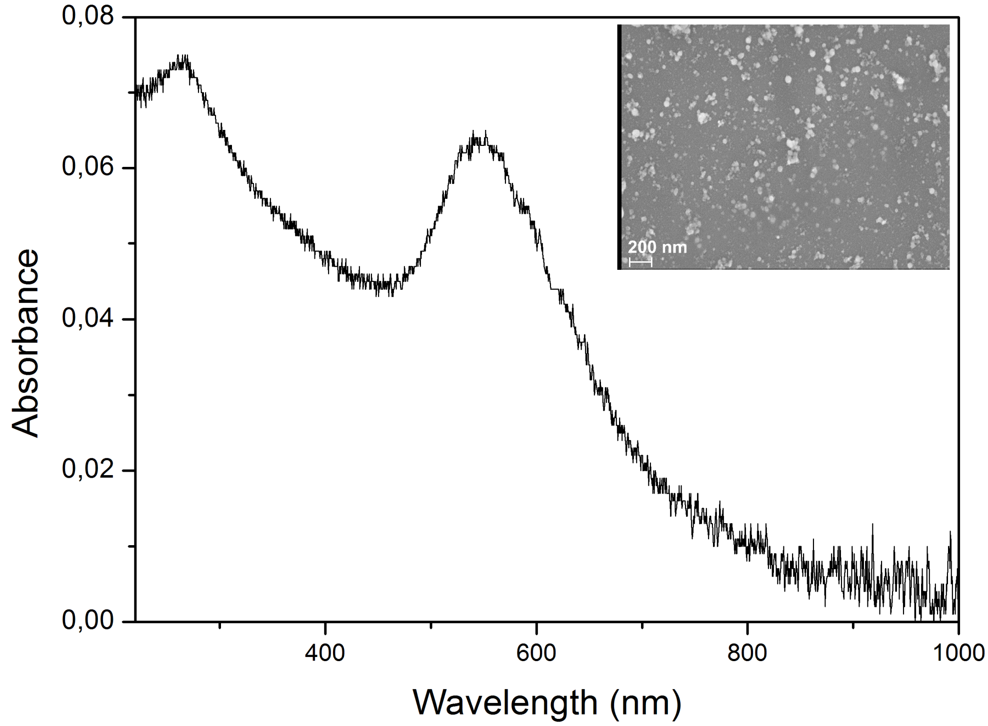
0,08
0,06
0,04
0,02
0,00
Absorbance
400
600
800
1000
Wavelength (nm)
200 nm

Fig.1

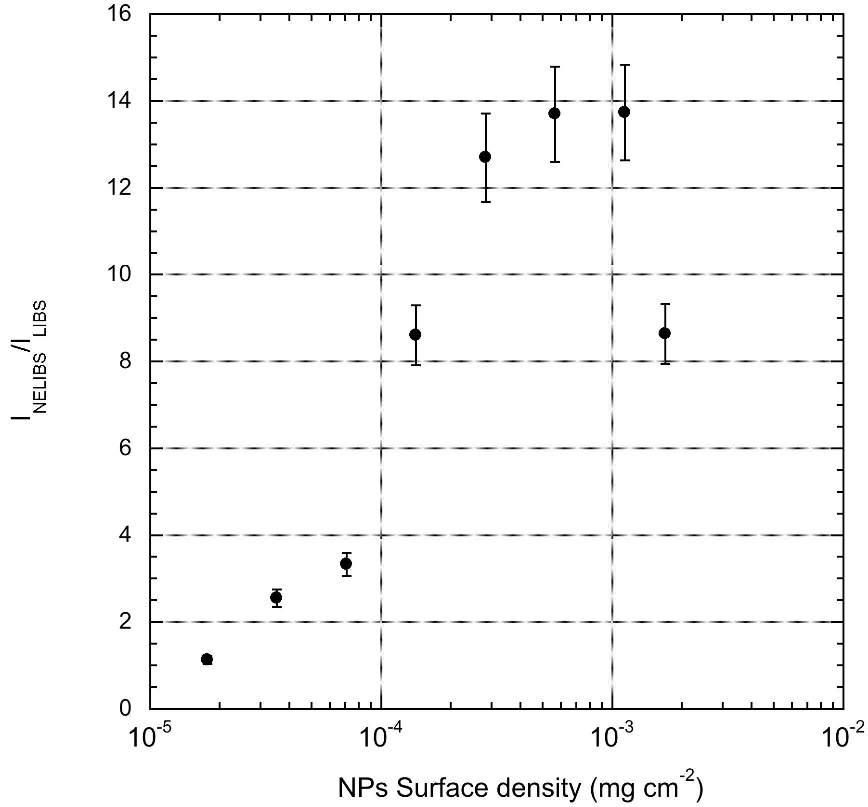
16
14
12
10
8
6
4
2
0
I_{NELIBS}/I_{LIBS}
10^{-5}
10^{-4}
10^{-3}
10^{-2}
NPs Surface density (mg cm^{-2})

FIG.2

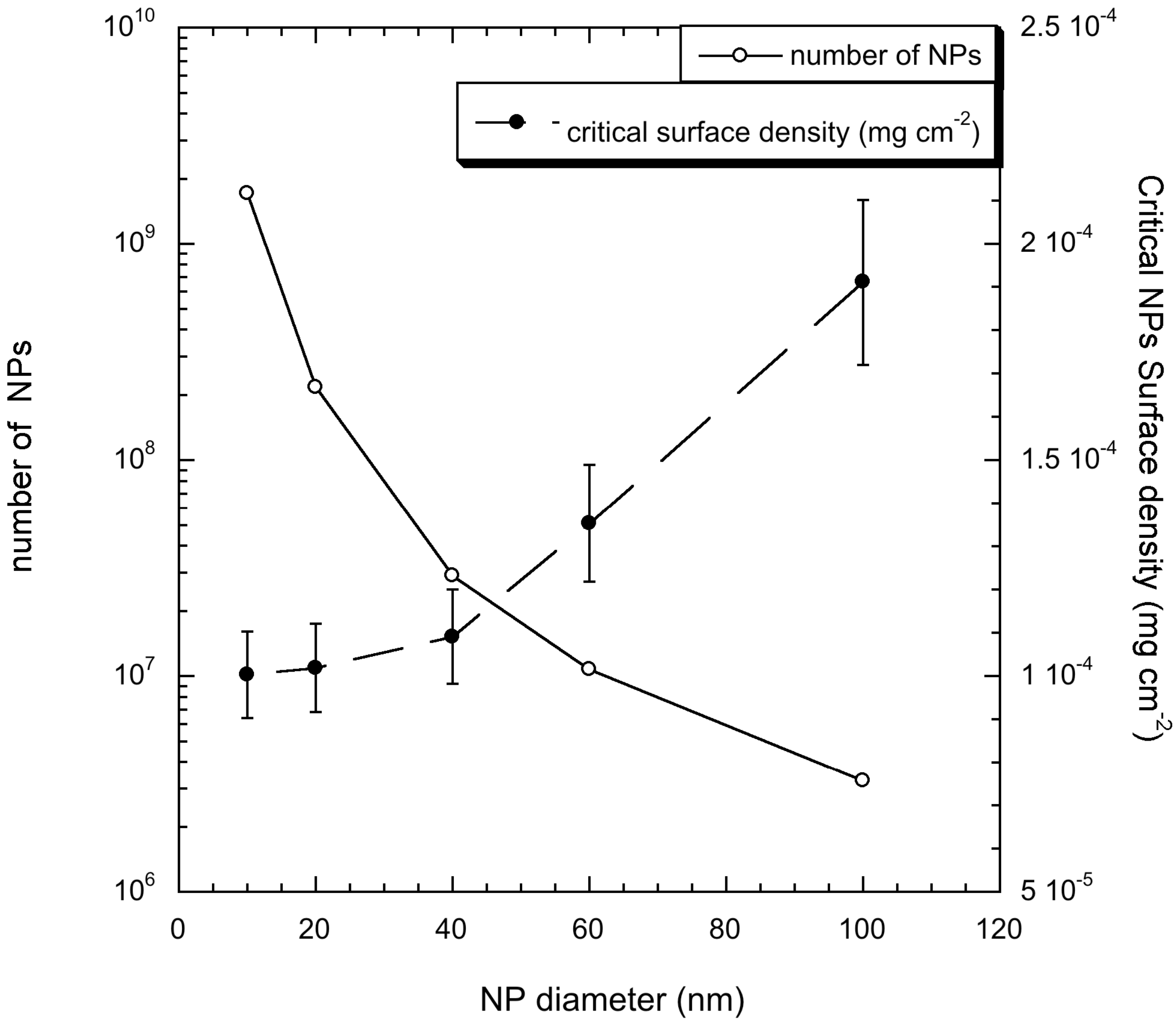

number of NPs
critical surface density (mg cm^{-2})
number of NPs
Critical NPs Surface density (mg cm^{-2})
NP diameter (nm)
10^{10}
10^{9}
10^{8}
10^{7}
10^{6}
2.5 10^{-4}
2 10^{-4}
1.5 10^{-4}
1 10^{-4}
5 10^{-5}
0
20
40
60
80
100
120

FIG.3

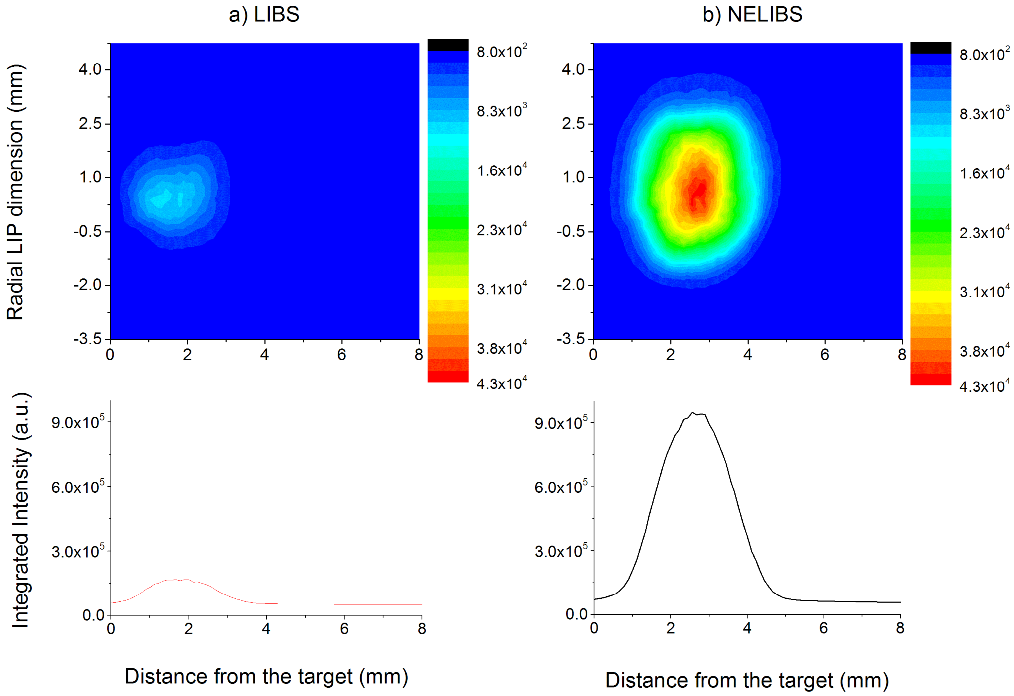
a) LIBS
b) NELIBS
Radial LIP dimension (mm)
4.0
2.5
1.0
-0.5
-2.0
-3.5
8.0x10^2
8.3x10^3
1.6x10^4
2.3x10^4
3.1x10^4
3.8x10^4
4.3x10^4
Integrated Intensity (a.u.)
9.0x10^5
6.0x10^5
3.0x10^5
0.0
0
2
4
6
8
Distance from the target (mm)
Distance from the target (mm)

FIG.4

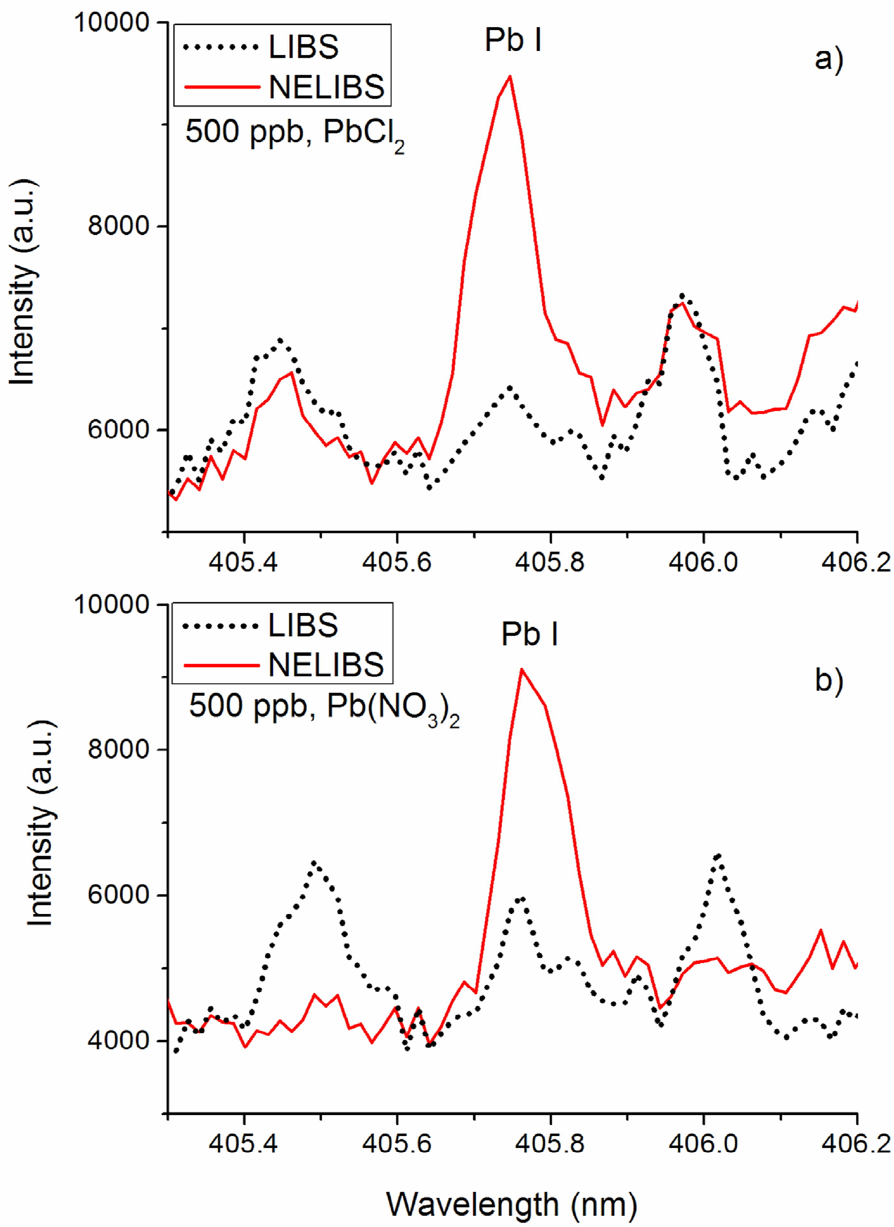

10000
8000
6000
Intensity (a.u.)
LIBS
NELIBS
500 ppb, $PbCl_2$
Pb I
a)
405.4
405.6
405.8
406.0
406.2
10000
8000
6000
4000
Intensity (a.u.)
LIBS
NELIBS
500 ppb, $Pb(NO_3)_2$
Pb I
b)
405.4
405.6
405.8
406.0
406.2
Wavelength (nm)

FIG.5a)-b)

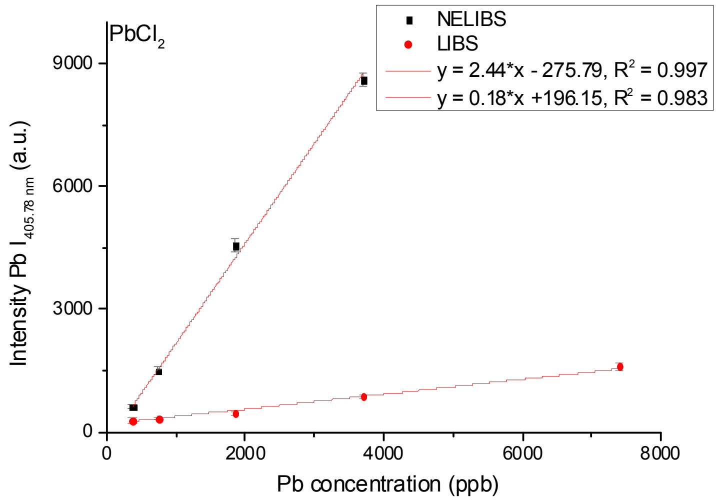
PbCl$_2$
NELIBS
LIBS
y = 2.44*x - 275.79, R^2 = 0.997
y = 0.18*x +196.15, R^2 = 0.983
Intensity Pb I$_{405.78\ nm}$ (a.u.)
Pb concentration (ppb)
0
3000
6000
9000
2000
4000
6000
8000

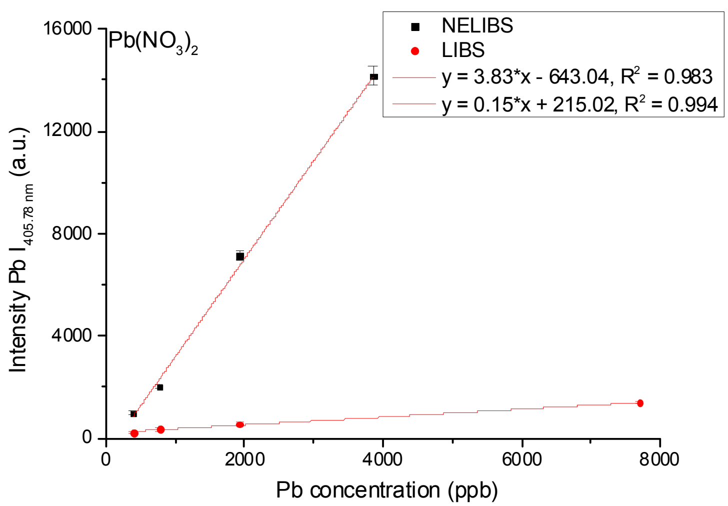
Pb(NO$_3$)$_2$
NELIBS
LIBS
y = 3.83*x - 643.04, R^2 = 0.983
y = 0.15*x + 215.02, R^2 = 0.994
Intensity Pb I$_{405.78\ nm}$ (a.u.)
Pb concentration (ppb)
0
4000
8000
12000
16000
2000
4000
6000
8000

FIG.6 a)-b)

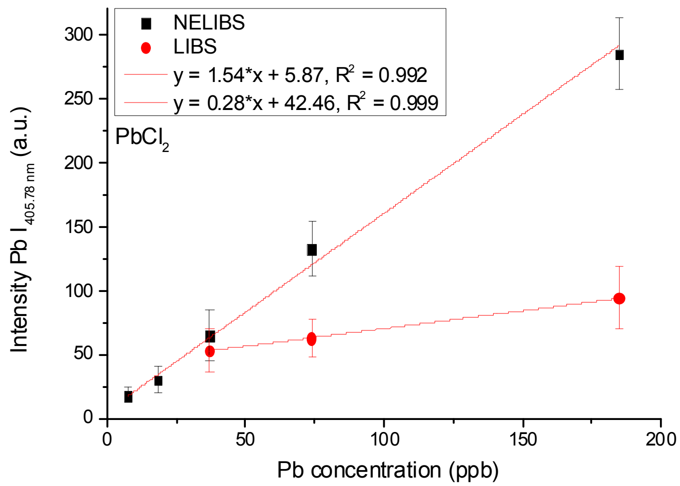
NELIBS
LIBS
y = 1.54*x + 5.87, R² = 0.992
y = 0.28*x + 42.46, R² = 0.999
PbCl2
Intensity Pb I405.78 nm (a.u.)
Pb concentration (ppb)
0
50
100
150
200
250
300

FIG.7

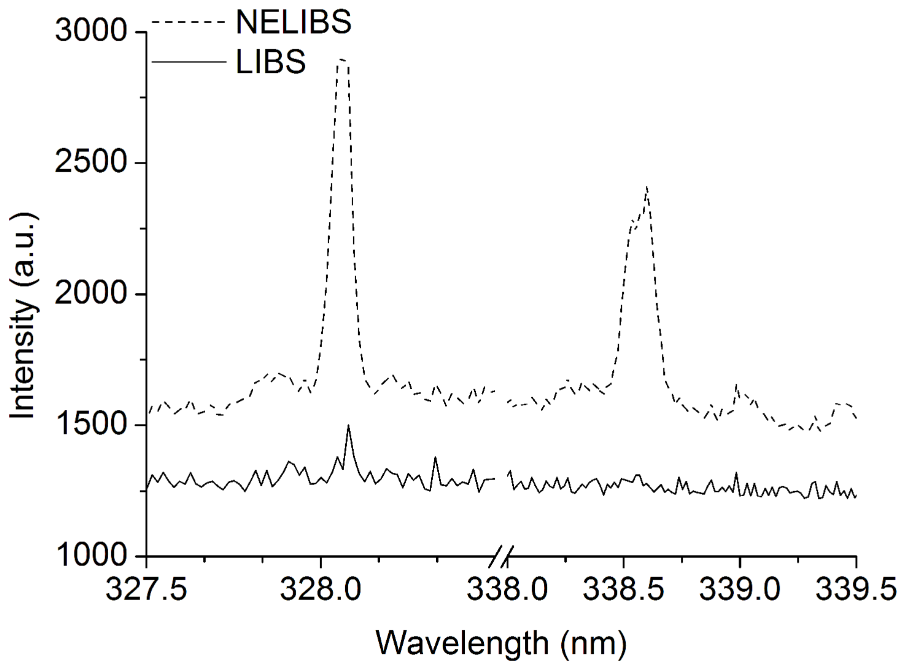
NELIBS
LIBS
3000
2500
2000
1500
1000
Intensity (a.u.)
327.5
328.0
338.0
338.5
339.0
339.5
Wavelength (nm)

FIG.8

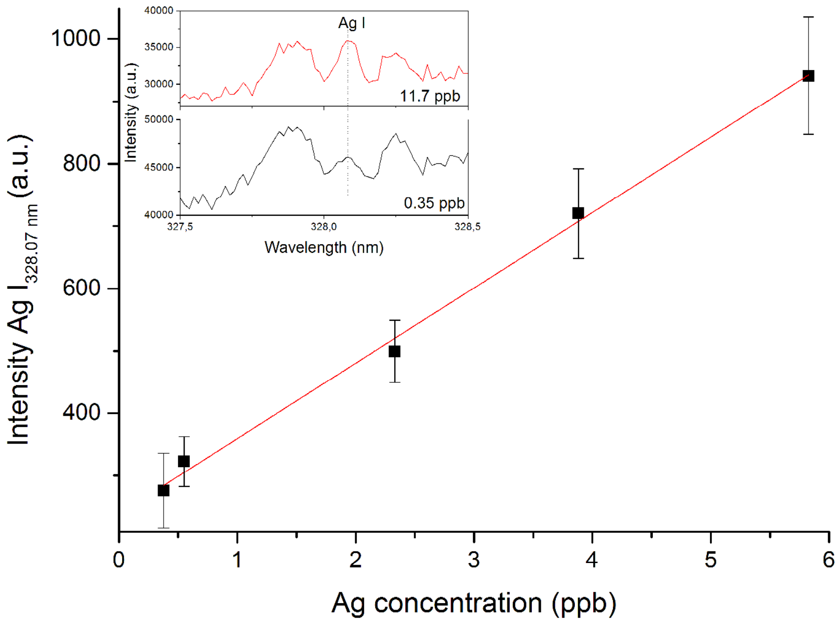

Intensity Ag I$_{328.07\ nm}$ (a.u.)
1000
800
600
400
0
1
2
3
4
5
6
Ag concentration (ppb)
Ag I
11.7 ppb
0.35 ppb
Intensity (a.u.)
Wavelength (nm)

FIG.9

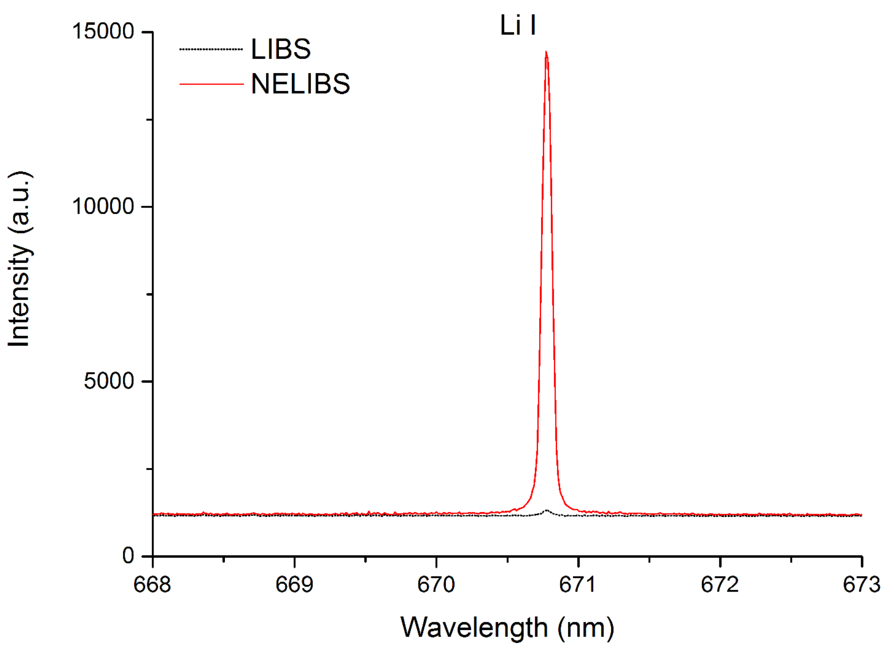
Li I
LIBS
NELIBS
Intensity (a.u.)
15000
10000
5000
0
668
669
670
671
672
673
Wavelength (nm)

FIG.10

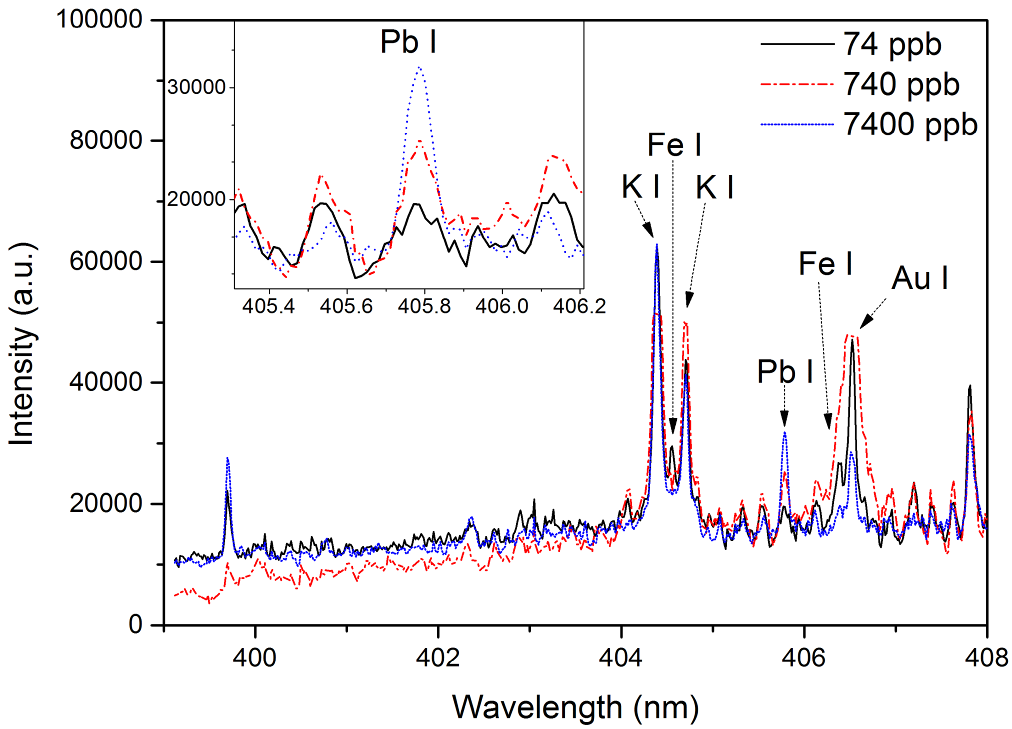
Pb I
74 ppb
740 ppb
7400 ppb
Fe I
K I
K I
Fe I
Au I
Pb I
Intensity (a.u.)
Wavelength (nm)
100000
80000
60000
40000
20000
0
400
402
404
406
408
30000
20000
405.4
405.6
405.8
406.0
406.2

FIG.11